



# Probing a dark photon using rare leptonic kaon and pion decays



Cheng-Wei Chiang<sup>a,b,c,\*</sup>, Po-Yan Tseng<sup>d</sup>

<sup>a</sup> Department of Physics, National Taiwan University, Taipei, 10617, Taiwan, ROC

<sup>b</sup> Institute of Physics, Academia Sinica, Taipei, 11529, Taiwan, ROC

<sup>c</sup> Physics Division, National Center for Theoretical Sciences, Hsinchu, 30013, Taiwan, ROC

<sup>d</sup> Kavli IPMU (WPI), UTIAS, The University of Tokyo, Kashiwa, Chiba 277-8583, Japan

## ARTICLE INFO

### Article history:

Received 29 December 2016

Received in revised form 8 February 2017

Accepted 9 February 2017

Available online 14 February 2017

Editor: J. Hisano

## ABSTRACT

Rare leptonic kaon and pion decays  $K^+(\pi^+) \rightarrow \mu^+ \nu_\mu e^+ e^-$  can be used to probe a dark photon of mass  $\mathcal{O}(10)$  MeV, with the background coming from the mediation of a virtual photon. This is most relevant for the 16.7-MeV dark photon proposed to explain a  $6.8\sigma$  anomaly recently observed in  ${}^8\text{Be}$  transitions by the Atomki Collaboration. We evaluate the reach of future experiments for the dark photon with vectorial couplings to the standard model fermions except for the neutrinos, and show that a great portion of the preferred 16.7-MeV dark photon parameter space can be decisively probed. We also show the use of angular distributions to further distinguish the signal from the background.

© 2017 The Authors. Published by Elsevier B.V. This is an open access article under the CC BY license (<http://creativecommons.org/licenses/by/4.0/>). Funded by SCOAP<sup>3</sup>.

## 1. Introduction

The search of new gauge interactions has been of great interest. Such efforts help us understand whether there is any other new force in Nature and how it fits to the grand picture of particle physics. If found, there is also a possibility that the new force carrier provides a portal between the standard model (SM) visible sector and a hidden sector involving new dynamics and matter contents.

In the simplest scenario, such a new vector boson may have an origin from some extra  $U(1)'$  gauge symmetry, under which some particles in both visible and hidden sectors are charged. It may even have kinetic or mass mixing with the SM photon or  $Z$  boson field to facilitate the mediation. After its symmetry breaking, as is often assumed, the  $U(1)'$  gauge boson acquires a mass and is commonly called the  $Z'$  boson if it is heavier than the electroweak scale or the dark photon if it is lighter. There have been a vast amount of studies on the neutral gauge boson over the years [1–11]. For example, recent direct searches at the LHC have already pushed the lower bound on the sequential  $Z'$  mass to about 3 TeV [12,13]. Further investigations rely on advances in the colliding energy and beam luminosity.

On the other hand, probes of the dark photon of mass below sub-GeV have been done using nuclear transitions [14–17] or

from its effects on the magnetic dipole moment of electron and/or muon [18–20]. The dark photon can be radiated off from some particle by bremsstrahlung and then decay into a pair of leptons in the fixed-target and beam-dump experiments [21–28]. With an appropriate coupling, it can be produced at  $e^+e^-$  colliders as well. If the dark photon couples to quarks, one can consider its production in meson decays, if kinematically allowed.

Recently, there is an elevated interest in the study of dark photon because of an experimental anomaly involved in isoscalar  ${}^8\text{Be}$  transitions reported by Krasznahorkay et al. [29]. In the transition from an excited state to the ground state, the nucleus emitted an electron–positron pair whose open angle and invariant mass were found to deviate from the SM expectation of internal pair creation (IPC) by  $6.8\sigma$ . It was shown that the distributions of open angle and invariant mass could be well fit by introducing a new particle with mass 16.7 MeV produced in the transition. In Refs. [30,31], the authors claimed that the new particle could be a vector boson  $X$  and provided the preferred ranges of its couplings with SM particles that were consistent with current dark photon search constraints. There are several analyses on how to further test the model in Ref. [30] using low-energy physical processes [32–34], as well as proposals of alternative models for the  ${}^8\text{Be}$  anomaly [35–41].

In this work, we propose to use rare leptonic decays of kaon and pion,  $K^+ \rightarrow \mu^+ \nu_\mu e^+ e^-$  and  $\pi^+ \rightarrow \mu^+ \nu_\mu e^+ e^-$ , as felicitous means to probe the light dark photon in the mass range of about  $\mathcal{O}(10)$  MeV, particularly in view of the putative gauge boson  $X$  with vectorial couplings mentioned above. This is because the final-state electron–positron pair production can be enhanced

\* Corresponding author.

E-mail addresses: [chengwei@phys.ntu.edu.tw](mailto:chengwei@phys.ntu.edu.tw) (C.-W. Chiang), [poyen.tseng@ipmu.jp](mailto:poyen.tseng@ipmu.jp) (P.-Y. Tseng).

via the mediation of the  $X$  boson over the SM background through a virtual photon. We show that the SM background and the signal have very different spectra in the  $e^+e^-$  invariant mass: the SM background has a continuous spectrum, whereas the decay through a dark photon features in a sharp resonance peak around the dark photon mass  $m_X$ . Moreover, the  $K^+ \rightarrow \mu^+ \nu_\mu e^+ e^-$  and  $\pi^+ \rightarrow \mu^+ \nu_\mu e^+ e^-$  decays are able to probe most part of the preferred coupling space inferred from the  $^8\text{Be}$  anomaly, assuming specific production rates of kaons/pions and their energy resolutions. We provide the projected experimental limits on the dark photon couplings based on these decay processes. We show that the signal events and SM background events have different behaviours in the  $\mu^+ \nu$  angular distribution in the leptonic kaon decay. We also discuss the influence of the kaon/pion structure dependence (i.e., the form factors), and find their effects almost irrelevant in current considerations.

This paper is organized as follows. In Section 2, we review the leptonic meson decays of interest to us. We present their decay amplitudes, including both inner bremsstrahlung and structure-dependent parts, and provide the form factors involved in the latter part. In Section 3, we consider the scenario that the dark photon has vectorial couplings to the SM fermions except for neutrinos, and three different experimental schemes for the kaon and pion decays. We estimate the projected reach in the dark photon couplings in Section 4. Numerical results are presented in Section 5, where we also discuss effects coming from the structure-dependent contributions. Our findings are summarized in Section 6.

## 2. The $K^+/\pi^+ \rightarrow \mu^+ \nu_\mu e^+ e^-$ decays via a dark photon and within the standard model

There can be many different ways to realize a light  $U(1)'$  gauge boson and let it couple with SM particles (directly or via mixing with the photon and/or  $Z$  boson). In the following, we will keep the formalism as general as possible, without explicitly referring to any particular new physics model. Suppose the gauge coupling  $e'$  of the dark photon  $X$  has a ratio of  $\varepsilon$  to the SM electric coupling, i.e.,  $e' = \varepsilon e$ . We denote the coupling charge of electron, muon,  $u, d, s$  quarks,  $K^+, \pi^+$  mesons, and proton and neutron with the  $X$  boson respectively by  $Q_{e, \mu, u, d, s, K^+, \pi^+, p, n}$ , whose values depend on the model.

In view of the analysis done in Refs. [30,31], we concentrate on the case where the dark photon  $X$  only possesses vectorial couplings in this work, and leave the possibility of an axial-vector boson to a future work. As detailed in Refs. [30,31], the putative gauge interaction is preferably protophobic for the  $^8\text{Be}$  anomaly [29] and has highly suppressed interactions with the electron neutrino, as constrained by the TEXONO experiment [42]. Two UV-complete models that could realize the above requirements were given in Ref. [31]. The  $X$  boson is associated with the  $U(1)_B$  group in one case and  $U(1)_{B-L}$  in the other, and mixes with the photon kinematically. In the former case, three vector-like pairs of color-singlet fields are introduced to cancel the gauge anomaly. In the latter case, gauge anomaly cancellation is achieved by adding to the SM three right-handed neutrinos. Besides, vector-like leptons are required to neutralize the neutrino couplings with the  $X$  boson. We refer interested readers to Ref. [31] for details. In the following analysis, we therefore assume the couplings between  $X$  and neutrinos to vanish identically. We will also focus on the region where  $|Q_p| < |Q_n|$ , although our analysis is more general.

The dark photon  $X$  can contribute to the

$$K^+(k) \rightarrow \mu^+(\ell) \nu_\mu(q) X(q') \rightarrow \mu^+(\ell) \nu_\mu(q) e^+(\ell_1) e^-(\ell_2)$$

decay, where the variables in the parentheses denote the momenta of the corresponding particles. The radiative kaon decay involves both inner bremsstrahlung (IB) and structure-dependent (SD) parts, and the total decay amplitude is given by [43–45]

$$i\mathcal{M}_K = \frac{G_F}{\sqrt{2}} V_{us}^* (\varepsilon e Q_{K^+}) \epsilon_\rho^*(q') \left[ f_K \bar{L}^\rho - \sqrt{2} \bar{H}^{\rho\mu} \ell_\mu \right], \quad (1)$$

where  $G_F$  is the Fermi decay constant,  $f_K = 155.6$  MeV is the kaon decay constant, the Cabibbo–Kobayashi–Maskawa (CKM) matrix element  $V_{us} \simeq 0.22538$ , and

$$\begin{aligned} \bar{L}^\rho &= m_\mu \bar{u}(q)(1 + \gamma_5) \\ &\quad \times \left\{ \frac{2k^\rho - q'^\rho}{2k \cdot q' - q'^2} + \left( \frac{Q_\mu}{Q_{K^+}} \right) \frac{2\ell^\rho + q'^\rho}{2\ell \cdot q' + q'^2} \right\} v(\ell), \\ \ell^\mu &= \bar{u}(q) \gamma^\mu (1 - \gamma_5) v(\ell), \\ \bar{H}^{\rho\mu} &= iV_1 \epsilon^{\rho\mu\alpha\beta} q'_\alpha k_\beta - A_1 (q' \cdot W g^{\rho\mu} - W^\rho q'^\mu) \\ &\quad - A_2 (q'^2 g^{\rho\mu} - q'^\rho q'^\mu) - A_4 (q' \cdot W q'^\rho - q'^2 W^\rho) W^\mu, \\ \epsilon_\rho^*(q') &= \frac{Q_e \varepsilon e}{q'^2 - m_X^2 + im_X \Gamma_X} \left[ \bar{u}(\ell_2) \gamma_\rho v(\ell_1) \right], \end{aligned} \quad (2)$$

with the  $\bar{L}^\rho$  part being due to IB, the  $\bar{H}^{\rho\mu}$  part containing the SD form factors  $V_1$  and  $A_{1,2,4}$ ,  $W^\mu \equiv k^\mu - q'^\mu$ ,  $q' \equiv \ell_1 + \ell_2$ , and  $\Gamma_X$  denoting the total width of  $X$ . The expressions in Eqs. (1) and (2) can be readily modified to give those for the SM background by replacing symbols associated with the dark photon by those for photon.

We follow the convention in Ref. [43] for the kaon form factors, which is consistent with the one used in Ref. [46].<sup>1</sup> We will set  $A_4 = 0$  because it has been found to be numerically negligible in comparison with the other form factors [44]. The rest form factors from recent measurements are parametrized as [47,48]

$$\begin{aligned} \sqrt{2} m_K A_1(q'^2, W^2) &= \frac{-F_A}{(1 - q'^2/m_\rho)(1 - W^2/m_{K_1})}, \\ \sqrt{2} m_K A_2(q'^2, W^2) &= \frac{-R}{(1 - q'^2/m_\rho)(1 - W^2/m_{K_1})}, \\ \sqrt{2} m_K V_1(q'^2, W^2) &= \frac{-F_V}{(1 - q'^2/m_\rho)(1 - W^2/m_{K^*})}, \end{aligned} \quad (3)$$

with  $F_A = 0.031$ ,  $R = 0.235$ ,  $F_V = 0.124$ ,  $m_\rho = 770$  MeV,  $m_{K_1} = 1270$  MeV, and  $m_{K^*} = 892$  MeV. Here we have assumed that the form factors for the leptonic kaon (and pion in the following case) decay from the dark photon exchange are the same as those from a photon exchange.

In the case of signal events, the distribution in the electron-positron invariant mass is a sharp resonance peak around  $m_X$ . The partial width of the dark photon decay into a pair of fermions is

$$\Gamma_{X \rightarrow f\bar{f}} = \frac{N_C m_X}{12\pi} \sqrt{1 - 4r_f} \times \left[ g_V^2 (1 + 2r_f) + g_A^2 (1 - 4r_f) \right], \quad (4)$$

where  $r_f = m_f^2/m_X^2$ ,  $N_C$  is the color factor, and  $g_V, g_A$  are the vector and axial-vector couplings between  $X$  and  $f$ . Taking  $m_X = 16.7$  MeV and assuming vectorial couplings as in Refs. [30,31], the dominant decay channel should be  $e^+e^-$ ,  $g_V = e \cdot \varepsilon \cdot Q_e$  and  $g_A = 0$ . For the SM background, one should set  $\varepsilon = 1$ ,  $Q_{K^+} = 1$ ,  $Q_\mu = -1$  and replace  $\epsilon^*(q')$  by

<sup>1</sup> We have compared three references [43,46,47] and decided to mainly follow the convention in Ref. [43]. It is consistent with Ref. [46] after taking into account an overall factor of  $-\sqrt{2}m_K$ , as explicitly shown in Eq. (C.8) of Ref. [43].

$$\epsilon_{\rho}^*(q') = \frac{e}{q'^2} [\bar{u}(\ell_2) \gamma_{\rho} v(\ell_1)]. \quad (5)$$

In this case, the electron–positron invariant mass distribution gives a continuous spectrum.

We also consider the pion decay  $\pi^+(k) \rightarrow \mu^+(\ell) \nu_{\mu}(q) X(q') \rightarrow \mu^+(\ell) \nu_{\mu}(q) e^+(\ell_1) e^-(\ell_2)$ . Similar to the kaon decay, the pion decay amplitude is [49,50]

$$i\mathcal{M}_{\pi} = \frac{G_F}{\sqrt{2}} V_{ud} (\varepsilon e Q_{\pi^+}) \epsilon_{\rho}^*(q') \{ f_{\pi} \bar{L}^{\rho} - \bar{H}^{\rho\mu} \ell_{\mu} \}, \quad (6)$$

with

$$\begin{aligned} \bar{L}^{\rho} &= m_{\mu} \bar{u}(q)(1 + \gamma_5) \\ &\times \left\{ \frac{2k^{\rho} - q'^{\rho}}{2k \cdot q' - q'^2} + \left( \frac{Q_{\mu}}{Q_{\pi^+}} \right) \frac{2\ell^{\rho} + q' \gamma^{\rho}}{2\ell \cdot q' + q'^2} \right\} v(\ell), \\ \ell^{\mu} &= \bar{u}(q) \gamma^{\mu} (1 - \gamma_5) v(\ell), \\ \bar{H}^{\rho\mu} &= i \frac{F_V}{m_{\pi}} \epsilon^{\rho\mu\alpha\beta} q'_{\alpha} k_{\beta} - \frac{F_A}{m_{\pi}} (q' \cdot k g^{\rho\mu} - k^{\rho} q'^{\mu}), \end{aligned} \quad (7)$$

where  $m_{\pi} = 139.57$  MeV,  $f_{\pi} = 130$  MeV is the pion decay constant, the CKM matrix element  $V_{ud} \approx 0.974$ , and the form factors [52]

$$\begin{aligned} F_V(\bar{q}^2) &= F_V(0) \times (1 + a\bar{q}^2), \\ F_A(\bar{q}^2) &= F_A(0), \end{aligned} \quad (8)$$

with  $F_V(0) = 0.0258$ ,  $F_A(0) = -0.0117$ ,  $a = 0.10$ , and  $\bar{q}^2 = 1 - (2E_X/m_{\pi})$ . We note that the form factors here are written such that we can directly quote the experimental results in Ref. [52]. Otherwise, they are identical to those in Eq. (2) when we make the correspondence

$$\frac{F_V}{m_{\pi}} \leftrightarrow V_1 \text{ and } \frac{F_A}{m_{\pi}} \leftrightarrow A_1 + A_2.$$

As in the kaon case, we have neglected the contribution of the form factor  $A_4$  here.

The IB term in the  $\pi^+ \rightarrow \mu^+ \nu e^+ e^-$  decay amplitude is proportional to  $m_{\mu}$ , therefore the IB contribution is more important than that in the  $\pi^+ \rightarrow e^+ \nu e^+ e^-$  decay amplitude. The SD contribution of the  $\pi^+ \rightarrow e^+ \nu e^+ e^-$  becomes more important at the kinematic regime of large  $e^+ e^-$  invariant mass [52].

### 3. Dark photon scenarios and search schemes

To explain the  $^8\text{Be}$  anomaly, the dark photon needs to have couplings with at least fermions in the first family except for the neutrino [29–31]. The preferred ranges of dark photon couplings are found to be [30]

$$\begin{aligned} |\varepsilon Q_n| &= (2 - 10) \times 10^{-3}, \\ |\varepsilon Q_p| &\lesssim 1.2 \times 10^{-3}, \\ |\varepsilon Q_e| &= (0.2 - 1.4) \times 10^{-3}, \end{aligned}$$

where the couplings are preferably protophobic in order to evade the constraints from the  $\pi^0 \rightarrow X\gamma$  decays measured at the NA48/2 experiment.

As alluded to in the previous section, two simple  $U(1)'$  models were explicitly constructed in Ref. [31] to give a protophobic  $X$  that has vanishing couplings with the neutrinos. In the example of  $U(1)_B$ ,  $Q_n \approx Q_e$  and  $Q_p$  is smaller; in the case of  $U(1)_{B-L}$ ,  $Q_n$  is bigger in magnitude than  $Q_p \approx -Q_e$ . Bearing these two specific examples in mind, we will treat  $Q_{p,n,e}$  as phenomenologically independent parameters to cover more general cases in

**Table 1**

Branching ratios of the SM background in the range of  $m_X - \frac{\delta m}{2} < m_{e^+e^-} < m_X + \frac{\delta m}{2}$ , where  $m_X = 16.7$  MeV, for different experimental schemes.

	Scheme 1	Scheme 2	Scheme 3
$\Delta\text{BR}_{\gamma^*}(K^+ \rightarrow \mu^+ \nu e^+ e^-)$	$2.54 \times 10^{-7}$	$1.29 \times 10^{-6}$	$2.70 \times 10^{-6}$
$\Delta\text{BR}_{\gamma^*}(\pi^+ \rightarrow \mu^+ \nu e^+ e^-)$	$1.61 \times 10^{-10}$	$8.69 \times 10^{-10}$	$2.21 \times 10^{-9}$

the following numerical analysis. With  $Q_u = (\frac{2}{3}Q_p - \frac{1}{3}Q_n)$  and  $Q_{d,s} = (\frac{2}{3}Q_n - \frac{1}{3}Q_p)$ , we have  $Q_{K^+} = Q_{\pi^+} = Q_p - Q_n$ .

Here we consider three different experimental schemes for the estimation of projected limits in the determination of dark photon gauge coupling. Suppose we produce  $N_{K^+, \pi^+}$  kaons and pions, respectively, and measure the  $e^+ e^-$  invariant mass from the decays with an energy resolution of  $\delta m$ . The schemes are<sup>2</sup>:

- **Scheme 1:**  $N_{K^+} = 10^{12}$ ,  $N_{\pi^+} = 10^{14}$ , and  $\delta m = 1$  MeV,
- **Scheme 2:**  $N_{K^+} = 10^{11}$ ,  $N_{\pi^+} = 10^{13}$ , and  $\delta m = 1$  MeV,
- **Scheme 3:**  $N_{K^+} = 10^{11}$ ,  $N_{\pi^+} = 10^{13}$ , and  $\delta m = 5$  MeV.

The energy resolution  $\delta m$  used here is much larger than the dark photon width for  $|e \varepsilon Q_e| \approx (0.2 - 1.4) \times 10^{-3}$ , as preferred by the  $^8\text{Be}$  anomaly [30,31]. Therefore, we cannot determine its width from the resonance peak in the  $e^+ e^-$  invariant mass distribution. But in contrast, SM background gives a continuous spectrum.

### 4. The projected limits

In this section, we estimate the projected limits for the  $U(1)'$  gauge coupling or, equivalently, the  $\varepsilon$  parameter for the above-mentioned three experimental schemes, following the steps outlined in Ref. [53].

First, we use the simple definition of standard deviation

$$\sigma = \frac{S}{\sqrt{B}}, \quad (9)$$

where  $S$  is the number of signal events, and  $B$  is that of background events. In the following, we will consider  $\sigma = 2$ , corresponding to about 95% confidence limit (C.L.). Base on the experimental schemes, we write down the ratio of  $S$  and  $B$  in terms of the branching ratios

$$\frac{S}{B} = \frac{\text{BR}_X(\varepsilon, m_X) \times N_{K^+}}{\Delta\text{BR}_{\gamma^*} \times N_{K^+}}, \quad (10)$$

where  $\text{BR}_X(\varepsilon, m_X)$  and  $\Delta\text{BR}_{\gamma^*}$  are the branching ratios of the leptonic kaon (or pion) decay through  $X$  and  $\gamma^*$ , respectively, with the requirement that the  $e^+ e^-$  invariant mass falls within the energy range:  $m_X - \frac{\delta m}{2} < m_{e^+e^-} < m_X + \frac{\delta m}{2}$ . With a fixed  $m_X$ ,  $\text{BR}_X(\varepsilon, m_X)$  is proportional to  $\varepsilon^2$  due to the Breit–Wigner description and  $[(q'^2 - m_X^2)^2 + m_X^2 \Gamma_X^2]^{-1} \simeq \frac{\pi}{m_X \Gamma_X} \delta(q'^2 - m_X^2)$ . Combining Eqs. (9) and (10), we obtain the  $2\sigma$  probing limit on the ratio

$$\varepsilon_{\text{limit}}^2 = \frac{2}{\sqrt{\Delta\text{BR}_{\gamma^*} \times N_{K^+}}} \times \frac{\tilde{\varepsilon}^2 \times \Delta\text{BR}_{\gamma^*}}{\text{BR}_X(\tilde{\varepsilon})}, \quad (11)$$

where  $\tilde{\varepsilon}$  can be any reasonable value, as long as  $\Gamma_X \ll \delta m$ . The branching ratios of SM background in various schemes are listed in Table 1.

In Fig. 1, we show  $\varepsilon_{\text{limit}}^2$  versus  $m_X$  in colored curves for the three experimental schemes from kaon (left plot) and pion (right

<sup>2</sup> Such kaon production and mass resolution may be achieved by the CERN NA62 experiment in a few years [51] or the rare kaon decay experiment at J-PARC if they also look at charged kaons. The numbers for pions are based upon the stopped pion experiment at PIBETA during 1999–2001 and in 2004 [52].

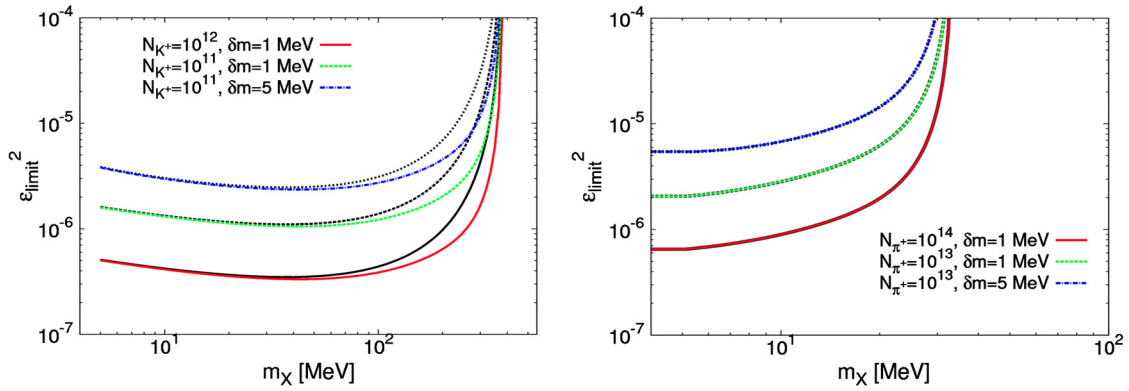


**Fig. 1.** Projected limits on  $\varepsilon$  with  $S/\sqrt{B} = 2$  (about 95% C.L.) with  $Q_{K^+, \pi^+} = 1$ , and  $Q_{e, \mu} = -1$ . The left panel is for the  $K^+$  decay, and the right panel is for the  $\pi^+$  decay. The red, green, and blue curves, including both IB and SD contributions, are for Schemes 1, 2, and 3, respectively. For each colored curve, the adjacent black curves include only the IB contribution. (For interpretation of the references to color in this figure legend, the reader is referred to the web version of this article.)

plot) decays by fixing  $Q_{K^+, \pi^+} = 1$  and  $Q_{e, \mu} = -1$ . We also show in black curves the effect of form factors on  $\varepsilon_{\text{limit}}^2$  by removing the SD part. For the dark photon mass of interest to the  $^8\text{Be}$  anomaly,  $m_X \sim 16.7$  MeV, the effects from kaon or pion form factors are basically negligible.

Before concluding this section, we comment on the decay length of the dark photon as produced from the kaon or pion decay. The decay length of  $X$  produced from  $K^+$  is  $\gamma_X \tau_X c$ , where  $\gamma_X$  is the boost factor,  $\tau_X = 1/\Gamma_{X \rightarrow ee}$  is the lifetime, and  $c$  is the speed of light. The largest boost factor from  $K^+ \rightarrow \mu^+ \nu X$  is  $\gamma_X \sim m_{K^+}/(2m_X) \sim 14.8$ . Taking the smallest value of  $\varepsilon Q_e = 0.2 \times 10^{-3}$  for the  $^8\text{Be}$  anomaly, the largest decay length of  $X$  with  $m_X = 16.7$  MeV is

$$\gamma_X \tau_X c \simeq 0.179 \text{ cm}.$$

Therefore, the dark photon should decay within the detector. On the other hand, a decay length of  $X$  of  $\sim 1$  cm corresponds to  $\varepsilon Q_e \sim 8.5 \times 10^{-5}$ .

## 5. Numerical results

Since the best-fit mass of dark photon for the  $^8\text{Be}$  anomaly is 16.7 MeV [29], we will fix  $m_X = 16.7$  MeV in the following discussions. Refs. [30,31] worked out the ranges of dark photon couplings with neutron, proton, and electron that could explain the  $^8\text{Be}$  anomaly and evade other experimental constraints. We will show how the leptonic kaon and pion decays can probe this region.

First, we take the experimental Scheme 1 and the rare leptonic kaon decay as an example. The SM background branching ratio is  $\Delta\text{BR}_{\gamma^*} = 2.54 \times 10^{-7}$ . Then the signal branching ratio corresponding to  $2\sigma$  upper limit of  $\varepsilon_{\text{limit}}$  is

$$\text{BR}_{\text{limit}} \equiv \varepsilon_{\text{limit}}^2 \times \frac{\text{BR}_X(\tilde{\varepsilon})}{\tilde{\varepsilon}^2} = 1.009 \times 10^{-9}. \quad (12)$$

Using  $\text{BR}_{\text{limit}}$  as a basic unit, we draw the contours of  $\text{BR}_X$  on the  $(\varepsilon Q_n, \varepsilon Q_p)$  parameter plane in Fig. 2. The black dotted line in the plot indicates the case where  $\varepsilon Q_{K^+} = 0$  and thus  $\text{BR}_X = 0$ . The region with  $\text{BR}_X < \text{BR}_{\text{limit}}$  is between the two red lines. This is the region where the dark photon cannot be checked using the leptonic kaon decay under the experimental Scheme 1. However, all the region outside the red contour, including most of the light green region, can be probed.

We perform a scan over the dark photon couplings,  $(\varepsilon Q_e, \varepsilon Q_p, \varepsilon Q_n)$ . In Fig. 3, we show the  $2\sigma$  projected limits for experimental Schemes 1, 2, and 3. Most part of the light green

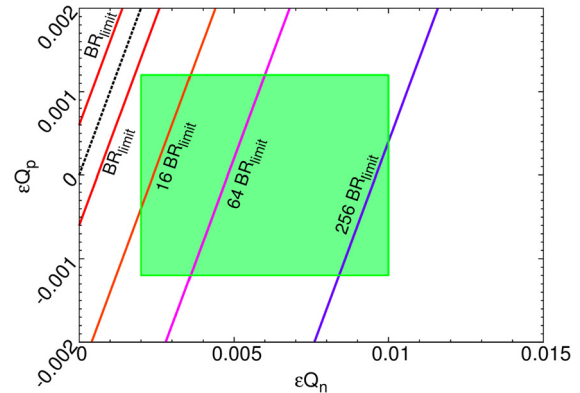


**Fig. 2.** Contours of  $\text{BR}_X$  on the  $\varepsilon Q_n$ - $\varepsilon Q_p$  plane. The light green area is the region favored by the  $^8\text{Be}$  anomaly [30,31]. The black dotted line is for  $\varepsilon Q_{K^+} = 0$ . The colored lines indicate the contours for various values of  $\text{BR}_X$ ; for example, the red contour is for  $\text{BR}_X = \text{BR}_{\text{limit}} = 1.009 \times 10^{-9}$ , where  $\text{BR}_{\text{limit}}$  comes from the experimental Scheme 1. (For interpretation of the references to color in this figure, the reader is referred to the web version of this article.)

area, outside the red, green, or blue regions, can be probed by the  $K^+ \rightarrow \mu^+ \nu e^+ e^-$  decay. In the left plot, the black dotted line indicates the case with  $Q_{K^+} = 0$ . In this case, the leptonic kaon decay loses sensitivity to probing the dark photon. In the right plot, the leptonic kaon decay also has less sensitivity to the dark photon along the semi-major axis of the ellipses. This is because when  $Q_{K^+} = -Q_{\mu^+}$ , a cancellation occurs in the IB amplitude and, therefore,  $\text{BR}_X$  is suppressed. When we turn off the SD contribution in the amplitude of leptonic kaon decay, virtually no noticeable change happens to Fig. 3. This demonstrates that uncertainties from the kaon form factors have little effects on the analysis, especially for  $m_X \simeq 16.7$  MeV.

In Fig. 4, we show the  $2\sigma$  projected limits from the  $\pi^+ \rightarrow \mu^+ \nu_\mu e^+ e^-$  decay as another possible probe. Comparing to Fig. 3, the projected limits from the leptonic pion decay are not as good. But a good portion of the preferred parameter region for the  $^8\text{Be}$  anomaly (light green area) can still be probed.

We now turn to the discussions of angular distributions of different subsystems in the  $\mu^+ \nu_\mu e^+ e^-$  final state. First, we show in Fig. 5 the distribution of  $\cos \theta_{e^+ e^-}^*$  from the leptonic kaon decay, where  $\theta_{e^+ e^-}^*$  denotes the angle of  $e^+$  with respect to the boost direction of  $X$ , but measured in the  $e^+ e^-$  center-of-mass frame. The parabolic shape of the angular distribution signifies the feature of vectorial couplings of the  $X$  boson and the photon, and it is almost independent of  $U(1)'$  charges and the SD part.

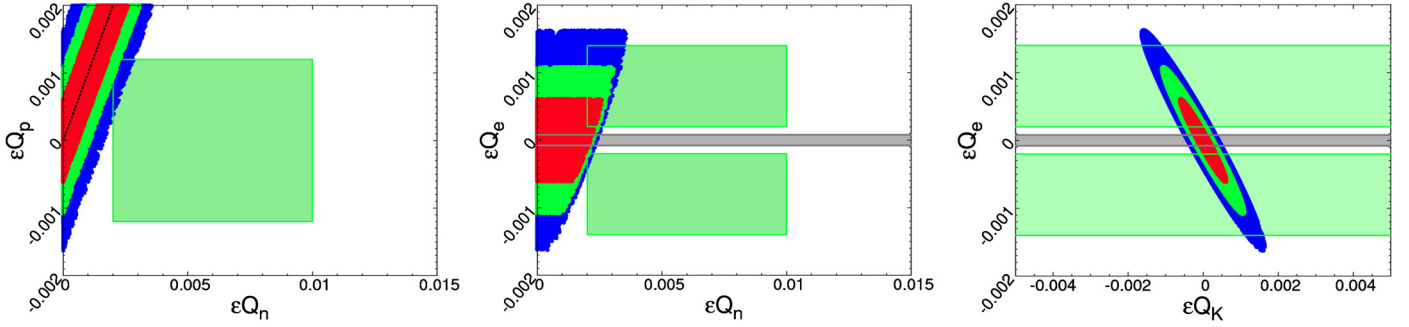


**Fig. 3.** The  $2\sigma$  projected limits from the  $K^+ \rightarrow \mu^+ \nu_\mu e^+ e^-$  decay under the experimental Scheme 1 (red), Scheme 2 (green), and Scheme 3 (blue). The light green area is the coupling region favored by the  ${}^8\text{Be}$  anomaly [30,31]. Depending on the schemes, the region outside the red, green, or blue areas are experimentally probe-able. The black dotted line in the left plot indicates the case with  $Q_{K^+} = 0$ . The grey regions in the middle and right plots indicate the possibility that the  $X$  has a decay length larger than 1 cm. (For interpretation of the references to color in this figure, the reader is referred to the web version of this article.)

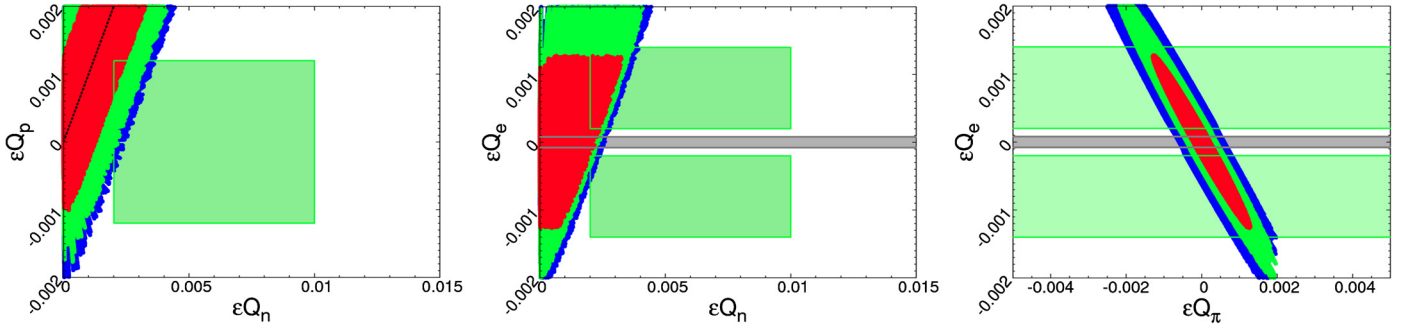


**Fig. 4.** Same as Fig. 3, but for the  $\pi^+ \rightarrow \mu^+ \nu_\mu e^+ e^-$  decay. The black dotted line in the left plot indicates the case with  $Q_{\pi^+} = 0$ . (For interpretation of the colors in this figure, the reader is referred to the web version of this article.)

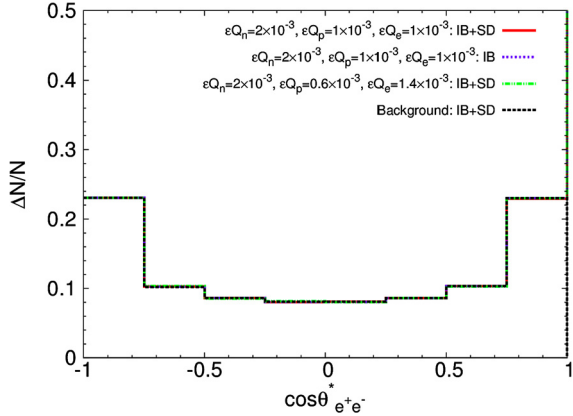


**Fig. 5.** Angular distribution of the  $K^+ \rightarrow \mu^+ \nu_\mu e^+ e^-$  decays, where  $\theta_{e^+e^-}^*$  denotes the angle of  $e^+$  with respect to the 3-momentum of  $X$ , but measured in the  $e^+e^-$  center-of-mass frame. The  $\Delta N/N$  is the ratio between the number of events within each bin to the total number of events. Virtually no difference can be seen among the four cases.

In Fig. 6, we show the distribution of  $\cos\theta_{\mu\nu}^*$ , where  $\theta_{\mu\nu}^*$  is the angle of  $\mu^+$  with respect to the boost direction of the  $\mu^+\nu$  system, but measured in the  $\mu^+\nu$  center-of-mass frame. In the left plot with two cases of different  $U(1)'$  charge assignments (with one more protophobic than the other), apparently the SM background and the signal from dark photon have the same behaviour as expected. In this case,  $\mu^+$  tends to fly along the direction of  $X$  in the  $K^+$  rest frame. In the right plot, we break up the different contributions by turning off specific  $U(1)'$  charges of particles in the decay process (thus the  $U(1)'$  charge is not conserved) and show the resulted angular behaviours. When  $\varepsilon Q_{K^+} \neq 0$  and  $\varepsilon Q_\mu = 0$ , we are left with only the first term in the curly brackets

of  $\bar{L}^\rho$  in Eq. (2) that has no angular dependence. When  $\varepsilon Q_{K^+} = 0$  and  $\varepsilon Q_\mu \neq 0$ , on the other hand, the second term in the curly brackets survives and has some minor angular dependence. When  $\varepsilon Q_{K^+} = -\varepsilon Q_\mu$ , the angle-independent parts cancel, rendering a more dramatic angular dependence, as shown by the blue-dotted histogram. The same cancellation also happens for the SM background, as the electric charges of  $K^+$  and  $\mu^-$  have opposite signs.

## 6. Summary

In this work, we propose to use the rare leptonic kaon and pion decays,  $K^+/\pi^+ \rightarrow \mu^+ \nu_\mu e^+ e^-$  to probe a light dark photon of  $\mathcal{O}(10)$  MeV mass. This is particularly suitable for probing the putative  $X$  gauge boson hinted at by the recent  ${}^8\text{Be}$  anomaly. We assume the scenario where the dark photon has vectorial couplings with the standard model fermions except for the neutrinos. We consider three schemes for the estimation of experimental reach. We estimate the projected limits by calculating the numbers of events from both dark photon and SM background. We perform a scan of dark photon couplings,  $(\varepsilon Q_e, \varepsilon Q_p, \varepsilon Q_n)$ , and compare the results with the region favored by the  ${}^8\text{Be}$  anomaly. Moreover, we show the angular distributions of final-state  $e^+e^-$  and  $\mu^+\nu$  systems in their own center-of-mass frames.

In general, Scheme 1 has the best sensitivity to probe the dark photon couplings due to a larger number of events as well as a better energy resolution. Most of the parameter space preferred by the  ${}^8\text{Be}$  anomaly can be probed by both  $K^+ \rightarrow \mu^+ \nu_\mu e^+ e^-$  and  $\pi^+ \rightarrow \mu^+ \nu_\mu e^+ e^-$  decays. The effects from kaon and pion form factors are found to be negligible in the projected limits for  $m_X = 16.7$  MeV. In each specific experimental scheme, the projected limits from the kaon decay are stronger than those from the pion decay. When  $K^+$  and  $\mu^-$  have opposite couplings with the dark photon, the signal events and the SM background events have

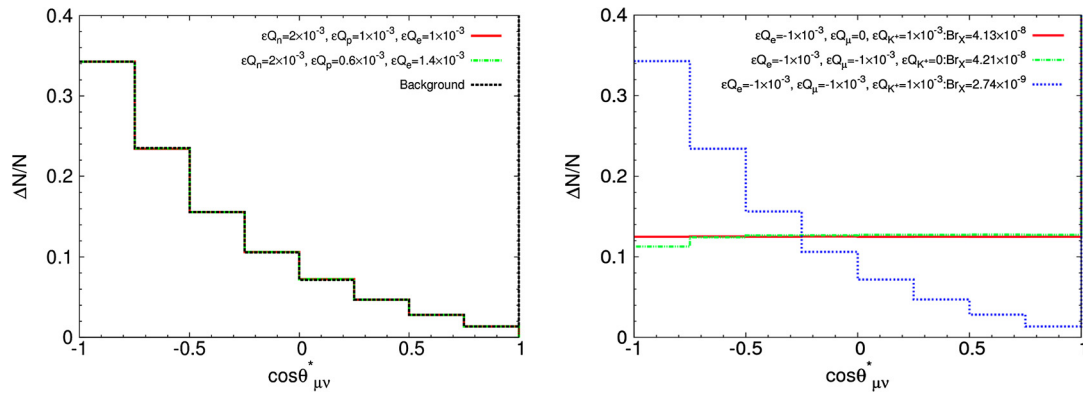


**Fig. 6.** The  $\cos\theta_{\mu\nu}^*$  distribution of the  $K^+ \rightarrow \mu^+\nu_\mu e^+e^-$  decays, where  $\theta_{\mu\nu}^*$  denotes the angle of  $\mu^+$  with respect to the  $\mu^+\nu$  3-momentum sum, but measured in the  $\mu^+\nu$  center-of-mass frame. Both IB and SD contributions are included in the calculations. The left plot compares two cases of different  $U(1)'$  charge assignments with the SM background. The right plot shows the behaviours of different contributions in the decay amplitude by turning off certain  $U(1)'$  charges. (For interpretation of the colors in this figure, the reader is referred to the web version of this article.)

the same behaviour in the  $\mu^+\nu$  angular distributions because the  $U(1)'$  charges of the particles in this process are proportional to their respective electric charges. The  $e^+e^-$  angular distribution can directly reveal the vectorial nature of the dark photon interaction.

### Acknowledgements

C.W.C would like to thank the hospitality of Kavli IPMU during his visit in 2016 summer, where this project was initiated. He is also indebted to B. Hsiung for discussions about experimental perspectives. This research was supported in part by the Ministry of Science and Technology of Taiwan under Grant No. MOST 104-2628-M-002-014-MY4, and in part by World Premier International Research Center Initiative (WPI), MEXT, Japan.

### References

- [1] A. Leike, *Phys. Rep.* 317 (1999) 143, arXiv:hep-ph/9805494.
- [2] P. Langacker, *Rev. Mod. Phys.* 81 (2009) 1199, arXiv:0801.1345 [hep-ph].
- [3] T.G. Rizzo, arXiv:hep-ph/0610104.
- [4] J. Erler, P. Langacker, S. Munir, E. Rojas, *J. High Energy Phys.* 0908 (2009) 017, arXiv:0906.2435 [hep-ph].
- [5] N. Borodatchenkova, D. Choudhury, M. Drees, *Phys. Rev. Lett.* 96 (2006) 141802, arXiv:hep-ph/0510147.
- [6] P. Fayet, *Phys. Rev. D* 75 (2007) 115017, arXiv:hep-ph/0702176.
- [7] B. Batell, M. Pospelov, A. Ritz, *Phys. Rev. D* 79 (2009) 115008, arXiv:0903.0363 [hep-ph].
- [8] R. Essig, P. Schuster, N. Toro, *Phys. Rev. D* 80 (2009) 015003, arXiv:0903.3941 [hep-ph].
- [9] M. Reece, L.T. Wang, *J. High Energy Phys.* 0907 (2009) 051, arXiv:0904.1743 [hep-ph].
- [10] R. Essig, et al., arXiv:1311.0029 [hep-ph].
- [11] J. Alexander, et al., arXiv:1608.08632 [hep-ph].
- [12] M. Aaboud, et al., ATLAS Collaboration, *Phys. Lett. B* 761 (2016) 372, arXiv:1607.03669 [hep-ex].
- [13] V. Khachatryan, et al., CMS Collaboration, arXiv:1609.05391 [hep-ex].
- [14] S.B. Treiman, F. Wilczek, *Phys. Lett. B* 74 (1978) 381.
- [15] M.J. Savage, R.D. Mckeown, B.W. Filippone, L.W. Mitchell, *Phys. Rev. Lett.* 57 (1986) 178.
- [16] A.L. Hallin, F.P. Calaprice, R.W. Dunford, A.B. McDonald, *Phys. Rev. Lett.* 57 (1986) 2105.
- [17] M.J. Savage, B.W. Filippone, L.W. Mitchell, *Phys. Rev. D* 37 (1988) 1134.
- [18] M. Pospelov, *Phys. Rev. D* 80 (2009) 095002, arXiv:0811.1030 [hep-ph].
- [19] H. Davoudiasl, H.S. Lee, W.J. Marciano, *Phys. Rev. D* 86 (2012) 095009, arXiv:1208.2973 [hep-ph].
- [20] M. Endo, K. Hamaguchi, G. Mishima, *Phys. Rev. D* 86 (2012) 095029, arXiv:1209.2558 [hep-ph].
- [21] H. Merkel, et al., A1 Collaboration, *Phys. Rev. Lett.* 106 (2011) 251802, arXiv:1101.4091 [nucl-ex].
- [22] S. Abrahamyan, et al., APEX Collaboration, *Phys. Rev. Lett.* 107 (2011) 191804, arXiv:1108.2750 [hep-ex].
- [23] J.D. Bjorken, R. Essig, P. Schuster, N. Toro, *Phys. Rev. D* 80 (2009) 075018, arXiv:0906.0580 [hep-ph].
- [24] J. Blumlein, J. Brunner, *Phys. Lett. B* 701 (2011) 155, arXiv:1104.2747 [hep-ex].
- [25] S.N. Gninenko, *Phys. Rev. D* 85 (2012) 055027, arXiv:1112.5438 [hep-ph].
- [26] S.N. Gninenko, *Phys. Lett. B* 713 (2012) 244, arXiv:1204.3583 [hep-ph].
- [27] S. Andreas, C. Niebuhr, A. Ringwald, *Phys. Rev. D* 86 (2012) 095019, arXiv:1209.6083 [hep-ph].
- [28] J. Blümlein, J. Brunner, *Phys. Lett. B* 731 (2014) 320, arXiv:1311.3870 [hep-ph].
- [29] A.J. Krasznahorkay, et al., *Phys. Rev. Lett.* 116 (4) (2016) 042501, arXiv:1504.01527 [nucl-ex].
- [30] J.L. Feng, B. Fornal, I. Galon, S. Gardner, J. Smolinsky, T.M.P. Tait, P. Tanedo, *Phys. Rev. Lett.* 117 (7) (2016) 071803, arXiv:1604.07411 [hep-ph].
- [31] J.L. Feng, B. Fornal, I. Galon, S. Gardner, J. Smolinsky, T.M.P. Tait, P. Tanedo, arXiv:1608.03591 [hep-ph].
- [32] L.B. Chen, Y. Liang, C.F. Qiao, arXiv:1607.03970 [hep-ph].
- [33] C.H. Chen, T. Nomura, *Phys. Lett. B* 763 (2016) 304, arXiv:1608.02311 [hep-ph].
- [34] F.C. Correia, S. Fajfer, *Phys. Rev. D* 94 (2016) 115023, arXiv:1609.00860 [hep-ph].
- [35] P.H. Gu, X.G. He, arXiv:1606.05171 [hep-ph].
- [36] T. Kitahara, Y. Yamamoto, arXiv:1609.01605 [hep-ph].
- [37] U. Ellwanger, S. Moretti, *J. High Energy Phys.* 1611 (2016) 039, arXiv:1609.01669 [hep-ph].
- [38] C.S. Chen, G.L. Lin, Y.H. Lin, F. Xu, arXiv:1609.07198 [hep-ph].
- [39] M.J. Neves, J.A. Helaÿel-Neto, arXiv:1609.08471 [hep-ph].
- [40] Y. Kahn, G. Krnjaic, S. Mishra-Sharma, T.M.P. Tait, arXiv:1609.09072 [hep-ph].
- [41] O. Seto, T. Shimomura, arXiv:1610.08112 [hep-ph].
- [42] M. Deniz, et al., TEXONO Collaboration, *Phys. Rev. D* 81 (2010) 072001, arXiv:0911.1597 [hep-ex].
- [43] J. Bijnens, G. Colangelo, G. Ecker, J. Gasser, in: 2nd DAPHNE Physics Handbook, 1994, pp. 315–389, hep-ph/9411311.
- [44] T. Beranek, M. Vanderhaeghen, *Phys. Rev. D* 87 (1) (2013) 015024, arXiv:1209.4561 [hep-ph].
- [45] C.E. Carlson, B.C. Rislow, *Phys. Rev. D* 89 (3) (2014) 035003, arXiv:1310.2786 [hep-ph].
- [46] m. Bychkov, G. D'Ambrosio, Particle Data Group, Form factors for Radiative Pion and Kaon Decay, in: C. Patrignani, et al. (Eds.), *Chin. Phys. C* 40 (10) (2016) 100001, <http://dx.doi.org/10.1088/1674-1137/40/10/100001>.
- [47] A.A. Poblaguev, et al., *Phys. Rev. Lett.* 89 (2002) 061803, arXiv:hep-ex/0204006.
- [48] T. Beranek, Theoretical Analysis of Hidden Photon Searches in High-Precision Experiments, PhD thesis (Mainz U.), Apr 2014.
- [49] D.A. Bryman, P. Depommier, C. Leroy, *Phys. Rep.* 88 (1982) 151.
- [50] E. Frlez, et al., *Phys. Rev. Lett.* 93 (2004) 181804, arXiv:hep-ex/0312029.
- [51] The NA62 collaboration, NA62 Technical Design Document, NA62-10-07, <https://cds.cern.ch/record/1404985>, 2010.
- [52] M. Bychkov, et al., *Phys. Rev. Lett.* 103 (2009) 051802, arXiv:0804.1815 [hep-ex].
- [53] R. Essig, P. Schuster, N. Toro, B. Wojtkowski, *J. High Energy Phys.* 1102 (2011) 009, arXiv:1001.2557 [hep-ph].